



Water, chloroform, acetonitrile, and atrazine adsorption to the amorphous silica surface studied by vibrational sum frequency generation spectroscopy

Nadia N. Casillas-Ituarte, Heather C. Allen*

Department of Chemistry, The Ohio State University, 100 W. 18th Avenue, Columbus, OH 43210, United States

ARTICLE INFO

Article history:

Received 21 April 2009

In final form 16 October 2009

Available online 21 October 2009

ABSTRACT

Vibrational sum frequency generation (VSFG) spectroscopy was used to examine the air–silica interface before, during, and after adsorption of water, chloroform, acetonitrile, and atrazine, an *s*-triazine molecule. Adsorption via the surface silanol sites was observed for all the compounds. Adsorption of chloroform and acetonitrile was weaker compared to water. Binding to the surface silanol groups was observed to be reversible for chloroform, acetonitrile, and atrazine. The standard free energy of adsorption, $\Delta G_{\text{abs}}^{\circ}$, of atrazine to the silica surface was determined to be -35 kJ/mol at 23 °C.

© 2009 Elsevier B.V. All rights reserved.

1. Introduction

Adsorption of molecules to the surface of metal oxides is an area of study that has application to materials and environmental sciences [1,2]. In this study, surface selective vibrational sum frequency generation (VSFG) spectroscopy was used to examine the air–solid interface of amorphous silica. We investigated the adsorption of water vapor as a first step of the characterization of the silica surface before solvent exposure at ambient conditions. The adsorption of chloroform and acetonitrile was also investigated. These solvents have lower affinity to the silica surface compared to water. Silica, chosen as a model system of mineral oxides found in the environment [3], was probed after adsorption of atrazine (6-chloro-N2-ethyl-N4-isopropyl-1,3,5-triazine-2,4-diamine, Fig. 1), an *s*-triazine herbicide. Atrazine is frequently detected in ground and surface waters as a consequence of its widespread use and moderate persistence in the environment [4]. Although retention of herbicides is strongly correlated to the organic fraction [5], when this fraction is less than 0.001 the adsorption to the inorganic fraction (mineral oxides) needs to be considered as contributing to the overall sorption process [3].

Amorphous silica has been studied extensively [6,7], including second harmonic spectroscopy studies pioneered by the Eisenthal and Geiger groups [8–11]; however there are few studies at the air–solid interface under ambient conditions with mid-range ($\sim 45\%$) relative humidity (RH) [12]. Silica is fully hydroxylated in water-saturated conditions [13]; yet in non water-saturated conditions (depending on the RH), there are a number of monolayers of water adsorbed on the surface [6]. Surface silanol groups [14] act

as adsorption sites for adsorbates capable of undergoing donor–acceptor interactions. Thus, surface silanol groups play a key role in sorption processes involving physical (including hydrogen bonding) and chemical bonding forces. The surface charge of a mineral is the consequence of the protonation–deprotonation of surface functional groups, mostly OH [15]. Far from the point of zero charge (PZC) at low or high pH, the surface charge is dependent on the pK_a 's of the oxide surface in addition to the solution ionic strength and the nature of the electrolyte in the solution. Ong et al. [8] studied the silica surface and measured the two pK_a 's using second harmonic generation. The pH at the point of zero charge (pH_{pzc}) reported for amorphous silica ranges from 2 to 3.5 [7,16,17]. The surface is positively charged at a $pH < pH_{\text{pzc}}$, and negatively charged at a $pH > pH_{\text{pzc}}$.

VSFG spectroscopy has become a highly versatile spectroscopic technique for the study of interfaces [12,18–25]. Under the electric dipole approximation, the VSFG intensity arises from noncentrosymmetric environments, such as at interfaces. VSFG is then forbidden in bulk phases where molecules experience a centrosymmetric environment. In contrast to Fourier transform infrared spectroscopy of silica after interaction with water [26,27], VSFG spectroscopy only probes the vibrational modes from water molecules adsorbed to the silica surface, where there is a lack of inversion symmetry. A significant advantage of VSFG over other surface techniques such as X-ray photoelectron spectroscopy and transmission electron microscopy is that VSFG can be used at different pressures including atmospheric.

The VSFG intensity, $I^{\omega_{\text{SFG}}}$, is proportional to the intensities of the infrared beam, $I^{\omega_{\text{IR}}}$, and visible beam, $I^{\omega_{\text{vis}}}$ as follows

$$I^{\omega_{\text{SFG}}}(\omega) \propto |\chi^{(2)}|^2 \cdot I^{\omega_{\text{IR}}} I^{\omega_{\text{vis}}} \quad (1)$$

where $\chi^{(2)}$ is the macroscopic nonlinear second-order susceptibility, which is described by a nonresonant term, $\chi_{\text{NR}}^{(2)}$, and the sum of the

* Corresponding author. Fax: +1 (614) 292 1685.

E-mail address: allen@chemistry.ohio-state.edu (H.C. Allen).

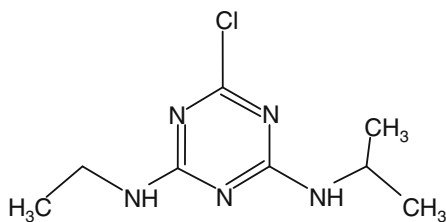


Fig. 1. Molecular structure of atrazine.

resonant terms, $\chi_v^{(2)}$. Amorphous silica bulk may contribute to $\chi_v^{(2)}$; however, its contribution is considered to be small [18]. $\chi_v^{(2)}$ is proportional to the molecular hyperpolarizability, β , the number density, and the molecular orientation. Additional details of VSFG theory can be found elsewhere [22,28].

2. Experimental

Atrazine (98%) (Fig. 1), chloroform (HPLC grade), and acetonitrile (>99.9%) were obtained from Riedel-de Haën (Germany), Sigma–Aldrich (PA, USA), and ACROS Organics (NJ, USA), respectively. Chemicals were used as received. Infrared-grade fused (amorphous) silica plates of 1.00 in. diameter and 0.188 in. thickness were obtained from Quartz Plus Inc. All glassware used was cleaned with $(\text{NH}_4)_2\text{S}_2\text{O}_8$ in H_2SO_4 solution (0.08 M) to eliminate trace organics and rinsed with Nanopure water (18.3 M Ω cm).

The silica plates were annealed in a muffle oven (Fisher Scientific, Isotemp Muffle Furnace) at 900 °C for 12 h to eliminate adsorbed organic substances. They were then cooled to room temperature for 30 min. Then spectra of the air–solid interface were acquired. These spectra are referred to as clean silica. Several silica plates were exposed to the laboratory RH conditions and stirred in water to monitor water (gas and liquid) adsorption prior to spectral acquisition in an open cell. Spectra of the air–solid interface of these silica plates were obtained at different exposure times (vapor adsorption) and after water evaporation. Spectra obtained in this way were highly reproducible. Pure solvents with different affinities for silica were used (water, chloroform, and acetonitrile). For these experiments, the silica plates were placed at $\sim 45^\circ$ inclination, then 100 μL of pure solvent was added dropwise to the surface in less than 1 min. For the atrazine exposure experiments, clean silica plates were placed vertically while stirring (to provide optimal mixing and surface exposure) solutions of atrazine in water (0.14 mM), chloroform (0.60 mM), or acetonitrile (0.55 mM). Desorption experiments were performed as described above, except that the silica plates were stirred in pure solvent (without atrazine). Spectra were acquired after the evaporation of the solvent. Surfaces were probed within two hours after exposure to solvents or atrazine solutions.

VSFG spectra of the air–silica interface were acquired from 2800 to 3900 cm^{-1} using a scanning VSFG spectrometer. The free silanol region ($\sim 3750 \text{ cm}^{-1}$) was also probed using a broad bandwidth VSFG spectrometer. Details of these two VSFG systems are described elsewhere [19,22]. The polarization combinations used for the scanning VSFG experiments was s, s, and p for the VSFG, 532 nm, and infrared beams respectively. Additional spectra shown in the Supplementary material were acquired under pss, ppp, and sps for the assignment of the atrazine CH vibrational modes (Table 1). All the spectra were acquired in ~ 45 min, unless otherwise indicated. The scanning spectra were normalized by the infrared profile, which was detected in real time with the VSFG intensity. The broadband spectra were normalized to the nonresonant signal from a GaAs crystal. Power dependence experiments

Table 1

VSFG spectral peak positions (cm^{-1}) of atrazine on silica. The subscript s denotes symmetric stretch, and as denotes asymmetric stretch. CH assignments are based on SFG spectral fits and comparison with ppp, sps, and pss polarization combinations (Supplementary material).

VSFG peak position (cm^{-1})	Spectral assignment
2884	$\text{CH}_3 \nu_s$
2919	$\text{CH} \nu_s$
2947	CH_3 Fermi resonance
2966	$\text{CH}_3 \nu_{as}$ in phase
2983	$\text{CH}_3 \nu_{as}$ out of phase

were conducted to ensure that the VSFG intensity was linearly correlated to the input energy of the visible and infrared beams (Eq. (1)). All the spectra were acquired at ~ 23 °C and at $47 \pm 8\%$ RH. An average of at least two replicate spectra is presented in all cases, and error bars show ± 1 standard deviation.

3. Results and discussion

The objective of this study is to understand how water and organic solvents influence atrazine adsorption to the amorphous silica surface. Adsorption of water in the gas and liquid phase on the surface was investigated. Additionally, solvents with lower affinity to the surface sites compared to water were used to further understand the competition for these sites.

3.1. Air–silica interface

Water vapor adsorption at the silica surface was investigated at ambient conditions ($\sim 40\%$ RH) to monitor the silica hydroxylation. Several spectra series of the air–silica interface expose to water vapor were acquired as a function of exposure time. In Fig. 2a and its inset one series is shown. A strong peak at 3750 cm^{-1} is observed and assigned to the free silanol stretch vibration ($\equiv \text{SiO-H}$) [29]. This peak intensity decreases over time. These results indicate that water vapor molecules interact with the surface silanol groups. The free silanol peak continues to be observed after 72 h (inset of Fig. 2a). Additionally, a small shoulder is observed at $\sim 3735 \text{ cm}^{-1}$, and is attributed to water weakly bound to silanol groups [30], somewhat similar to a ‘silica–gel’ structure [31].

After 24 h a broad band at $3000\text{--}3600 \text{ cm}^{-1}$ is also observed and assigned to hydrogen bonded OH stretching modes. The precise assignment within this broad band remains controversial [19,22,32–34]. This region intensity increases with increasing exposure time. The interfacial structure of adsorbed water on a surface can be found by the analysis of the two spectral bands at ~ 3200 and 3400 cm^{-1} corresponding to the stretching modes of the ordered, and the less ordered hydrogen bonded water, respectively [25]. These bands have also been reported as strongly and weakly hydrogen bonded water molecules, respectively [22,25]. After 24 h both bands are observed. Further exposure results in an increase in the intensity of only the 3400 cm^{-1} band. Others have observed using FTIR a combination of ordered and disordered layers with a dominance of ordered water on silicon dioxide and oxide surfaces after adsorption of water vapor at $\sim 40\%$ RH [35,36]. Others, using SFG, also observed a slight dominance of the 3200 cm^{-1} band at neutral pH indicative of an ordered interfacial water structure at the liquid water–silica (and quartz) interface; the ordering was highly dependent on surface ionization and therefore pH [21,24]. In our study the pH was ~ 6.5 , at which the surface is negatively charged ($\text{pH} > \text{pH}_{\text{pzc}}$), although the majority of the surface groups are expected to be SiOH groups [15]. We observe a combination of ordered and disordered hydrogen

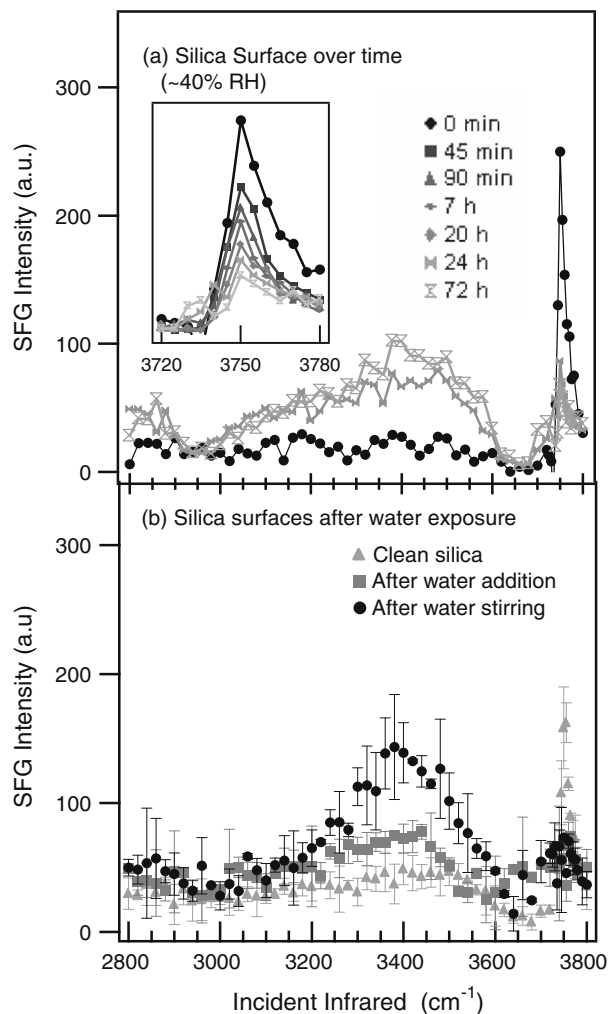


Fig. 2. VSFG spectra of silica at the air–solid interface: (a) at time intervals of exposure to ambient conditions (RH \sim 40%, 23 °C) and (b) after liquid water exposure.

bonded water after 24 h as shown in Fig. 2a. However, we observe a small enhancement of the 3400 cm^{-1} band after 72 h that suggests disordered hydrogen bonded water molecules are adsorbed with subsequent water exposure. The intensity enhancement of the 3400 cm^{-1} band suggests that water adsorbs to silanol-bound water and forms clusters rather than a uniform film [6,37]. Adsorption of water to water is more energetically favorable relative to adsorption of water to silica [38,39]. Cluster formation is typical of surfaces that are partially hydrophobic [6,7,37,38]. This surface structure is rather stable as evidenced by the highly reproducible spectra.

The square root of the VSFG intensity is proportional to the number of oscillators at the interface. The reduction in the free silanol intensity shown in the inset of Fig. 2a is assigned to a reduction in the number density since the average orientation of the free silanols is relatively constant over time, with a calculated angle of $26^\circ \pm 2$ from the surface normal (Supplementary material). Fig. 3 shows the relative free silanol percentage as a function of time (h). To determine the free silanol percentage, it was assumed that at time zero (Fig. 2a, ‘0 min’ spectrum) 100% of the silanol groups were free. Error bars show the standard deviation in the calculated percentage from different silica plates. The water adsorption follows two regimes, a fast component (<20 h) and a linear compo-

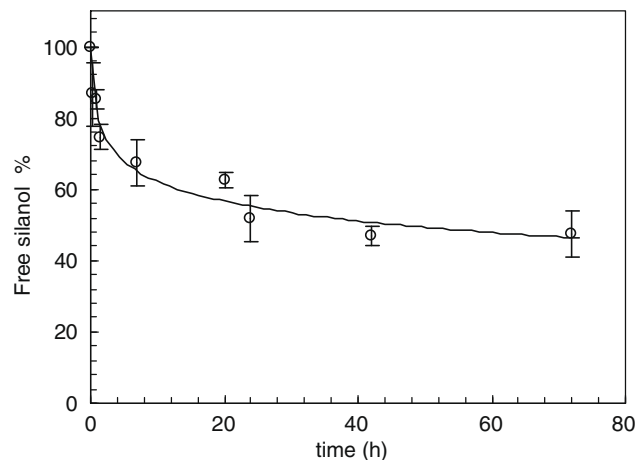


Fig. 3. Free silanol percentage as a function of time (h). The error bars are ± 1 standard deviation from the free silanol percentages obtained from different samples.

nent (>20 h). In the fast regime, the formation of clusters occurs [37].

The 3000–3600 cm^{-1} intensity can be modified by hydroxylation of the siloxane (Si–O–Si) groups. These are generated by the cleaning procedure of the silica plates, which includes heat treatment at 900 °C in air. The hydroxylation of surface siloxane groups generates an increased number of silanol groups that could subsequently interact with water vapor. Under our experimental conditions, complete hydroxylation to regenerate the initial silica surface is not expected [40].

To examine further the time dependency of water adsorption to the surface, spectra of the air–silica interface after addition of liquid water (exposure <1 min), and stirring in water (exposure ~ 30 min) were obtained as shown in Fig. 2b. A clean air–silica spectrum is also shown. Upon liquid water dropwise addition, the spectrum reveals a pronounced decrease of the silanol peak, and an enhancement in the hydrogen bonded OH region (3000–3600 cm^{-1}). This spectrum is similar to the spectra of water vapor adsorption shown in Fig. 2a. The spectrum obtained after stirring in water shows a decrease in the 3650 cm^{-1} region, and an increase in the 3400 cm^{-1} region relative to the water dropwise addition spectrum. The intensity of the 3200 cm^{-1} band in both spectra is similar. As described earlier, the higher intensity of the 3400 cm^{-1} band is the result of the incorporation of more disordered hydrogen bonded water molecules. Both spectra show an increase in the 3650–3740 cm^{-1} region which we assign to water weakly bound to silanol groups and vicinal pairs of isolated silanol [27,30]. There is also a possible contribution from the free OH stretch of water (observed at 3700 cm^{-1}), water dimers, and weakly hydrogen bonded water [41,42]. The silica surface hydration evolves in time. In the environment, mineral surfaces tend to hydrolyze resulting in the dissolution of the surface species to form bulk silicic acid and therefore exposing new silicon atoms [7].

3.2. Silica exposed to atrazine aqueous solution

A spectrum of the air–silica interface after stirring in atrazine aqueous solution (pH ~ 6.5) was obtained (Fig. 4d). The clean air–silica spectrum (solid line) along with the spectrum of silica after exposure to water (liquid) are also shown (Fig. 4a). After aqueous atrazine exposure, the spectrum reveals an intensity decrease of the silanol peak accompanied by an intensity increase in the 3100–3550 cm^{-1} region. The enhancement is primarily attributed to hydrogen bonded OH stretching modes. NH stretch-

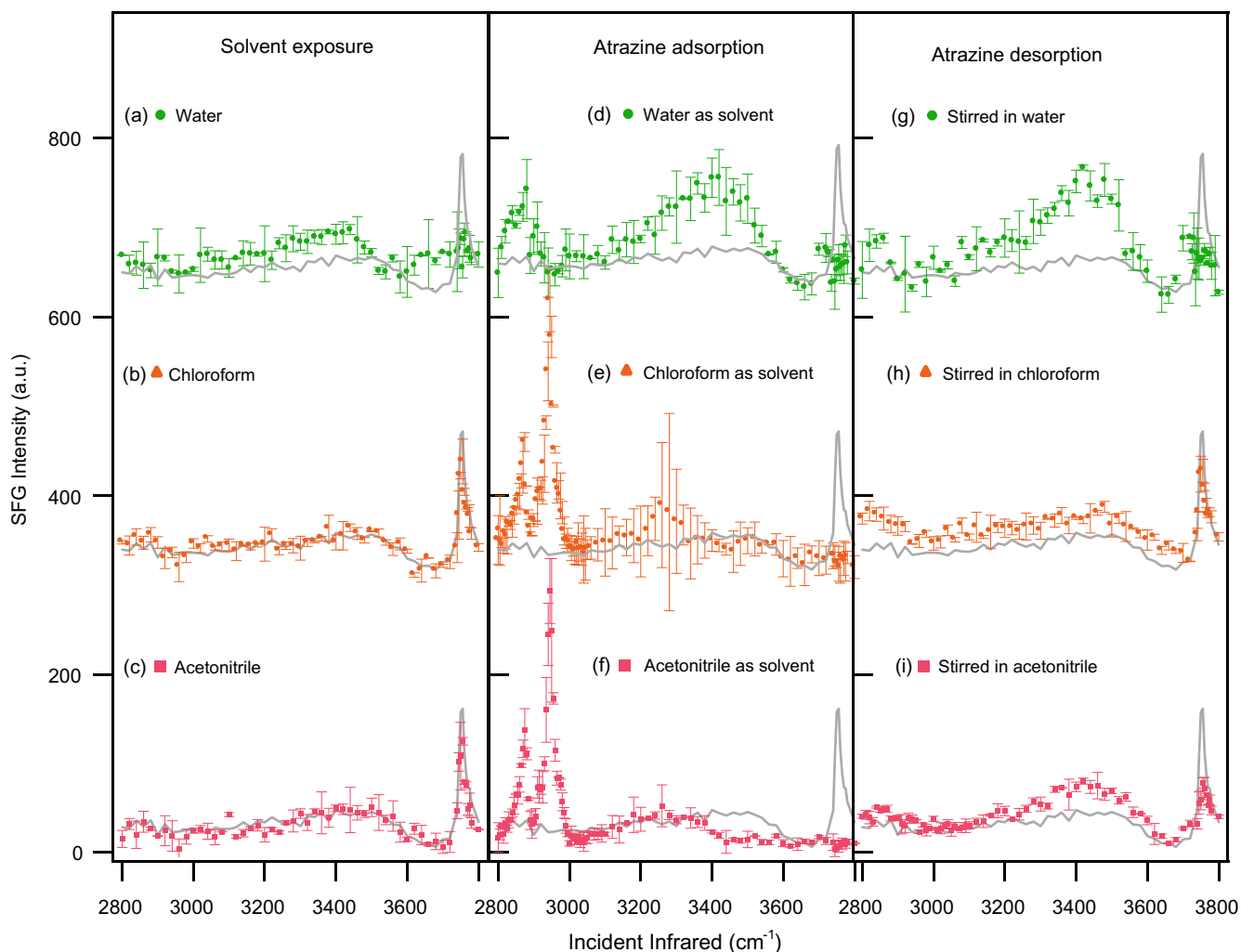


Fig. 4. VSFG ssp polarized spectra of silica at the air–solid interface after exposure to (a) water, (b) chloroform, and (c) acetonitrile, and exposure to atrazine solutions in (d) water, (e) chloroform, and (f) acetonitrile, and being stirred in (g) water, (h) chloroform, and (i) acetonitrile after atrazine exposure. The gray lines are the clean silica spectra for reference.

ing vibrations may contribute to the total VSFG intensity in this region. These results, and their similarity to Fig. 2b, suggest that the enhancement is dominated by water adsorption. However, a weak and broad peak is observed at $\sim 2900\text{ cm}^{-1}$ and is assigned to the atrazine CH stretching modes revealing that atrazine is adsorbed to the silica surface. At $\text{pH} \sim 6.5$, atrazine is a neutral molecule ($\text{p}K_{a1} = 1.65$ and $\text{p}K_{a2} = 1.95$) [43] and the silica surface is mostly terminated with silanol groups. This suggests that atrazine is physisorbed to silanol groups and/or surface water.

3.3. Silica exposed to atrazine in chloroform, and acetonitrile solutions

To address the experimental issue of low aqueous solubility (33 mg L^{-1} [44]), chloroform (52 g L^{-1} [44]) and acetonitrile were used as atrazine solvents. These two solvents provide additional insight into atrazine adsorption on silica since these solvents have different hydrogen bond affinities to the surface relative to that of water.

Solvent interaction with the surface was investigated by acquiring spectra of the air–silica interface after exposure to chloroform and acetonitrile (Fig. 4b and c). A spectrum of the air–silica surface before exposure to each solvent is also shown (solid line). After addition of chloroform or acetonitrile to the surface, the spectra reveal similar features to the clean silica spectrum, the broad band at

$3000\text{--}3600\text{ cm}^{-1}$ and the free silanol stretch peak at 3750 cm^{-1} . No peaks were observed in the CH region ($\sim 2900\text{ cm}^{-1}$). This indicates that chloroform and acetonitrile do not form stable complexes with the surface silanol groups under these experimental conditions.

Silica plates were placed in continuously stirring solutions of atrazine in chloroform and acetonitrile for one hour. Spectra were acquired after complete evaporation of the solvent (Fig. 4e and f). The free silanol peak at 3750 cm^{-1} is completely suppressed after the addition of both atrazine solutions. Also, in these figures a slight enhancement in the $3100\text{--}3400\text{ cm}^{-1}$ region relative to the 3500 cm^{-1} region is observed. This broad feature is significantly red shifted compared to the intensity observed in the after water only exposure (Fig. 4a). This red shifted feature is assigned to NH modes of atrazine (Raman spectrum of pure atrazine reveals this broad band, data not shown). Fig. 4e and f also show CH stretching modes attributed to atrazine adsorption (Table 1 and Supplementary material). Recall that CH stretching peaks from chloroform and acetonitrile were not detected (Fig. 4b and c).

Different silica plates were stirred in $0.01\text{--}0.55\text{ mM}$ atrazine solutions of acetonitrile. Spectra of the air–silica interface were obtained in the CH region (Fig. 5a) and the free silanol region (Fig. 5b). A clean silica surface spectrum is also shown. The spectra reveal that as the atrazine concentration increases, the intensity of

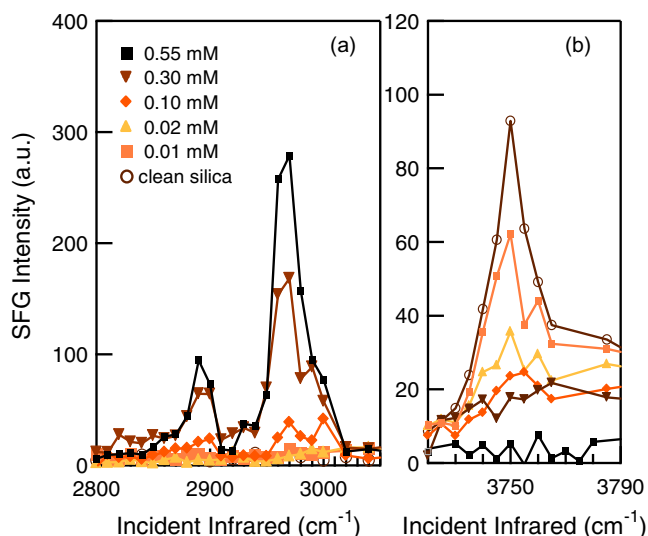


Fig. 5. VSFG ssp polarized spectra of the air–silica interface after exposure to 0.01, 0.02, 0.10, 0.30, and 0.55 mM atrazine solutions in acetonitrile in (a) the CH stretching and the (b) free silanol regions.

the CH region increases. Moreover, the signal in the free silanol region decreases with increasing atrazine concentration. The correlation of atrazine concentration to intensity loss of the free silanol peak strongly suggests that the silica surface interacts with atrazine through these functional groups.

It is likely that the atrazine–silica interaction involves the atrazine NH groups binding directly to the surface silanol groups through hydrogen bonding. This is supported by FTIR studies that showed hydrogen bond formation between surface silanol groups and weakly basic molecules [45,46]. In addition, the hydrogen bonding propensity of atrazine has been revealed by NMR studies, that is, atrazine molecules have been shown to accept hydrogens through hydrogen bonding with alcohols [47].

Atrazine adsorption was analyzed in terms of a Langmuir adsorption model described in detail by Mifflin et al. [11]. The inverse of the relative surface coverage as a function of the inverse atrazine concentration is shown in Fig. 6. It was assumed that the intensity reduction of the free silanol peak is only due to atrazine adsorption. From a linear least squares fit to the data, the

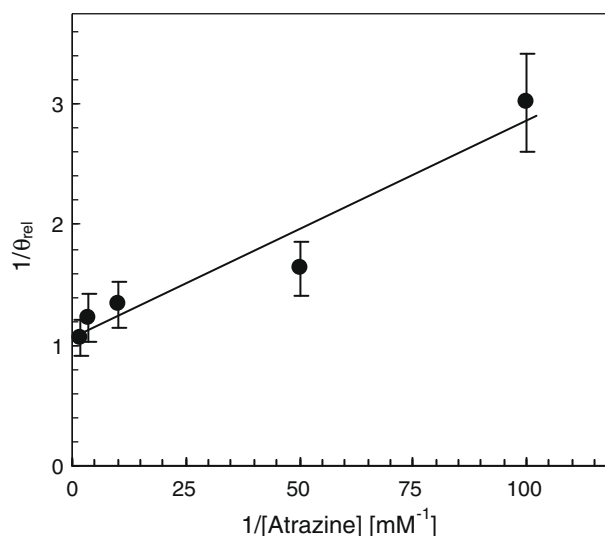


Fig. 6. The inverse of the silica surface coverage (θ) as a function of the inverse of the atrazine concentration in units of mM^{-1} .

slope of the resulting straight line reveals the equilibrium constant for atrazine adsorption K_{ads} to be $1.9 \times 10^6 \text{ M}^{-1}$ (details in the Supplementary material). The corresponding standard free energy of adsorption, $\Delta G_{\text{abs}}^\circ$, is found to be -35 kJ/mol at 23°C which is consistent with the formation of one to two hydrogen bonds and a weak physisorption process [7].

3.4. Silica exposed to water, chloroform, and acetonitrile after atrazine exposure

To further elucidate the interactions between atrazine and the surface silanol groups another series of experiments was performed. After the silica samples were exposed to atrazine (Fig. 4d–f), these same samples were then stirred in the corresponding pure solvent (Fig. 4g–i). The spectrum of the clean silica surface is also plotted in these figures.

The spectrum of the air–silica interface of atrazine adsorption after water stirring (Fig. 4g) reveals reduced intensity in the CH stretching region, which is consistent with the pure water adsorption spectra in Fig. 2. Lower intensity of these peaks suggests that atrazine has been removed from the surface. An increase in the hydrogen bonded region ($3000\text{--}3600 \text{ cm}^{-1}$) compared to the silica reference spectrum is also observed. This suggests that water molecules have aggregated at the surface. The slight increase in the free silanol peak relative to Fig. 4d (atrazine adsorbed) indicates that upon atrazine desorption, a fraction of the silanol groups are now free. Therefore, from studying the adsorption and desorption spectra, atrazine adsorption on silica involves relatively weak physical forces, that is, weak hydrogen bonding.

There are two possible mechanisms for the atrazine removal from the silica surface. First, displacement of atrazine molecules by water molecules can occur. This is suggested since water has a higher affinity for the surface silanols than atrazine; water forms stronger hydrogen bonds with the surface silanol relative to atrazine. Second, solvation of atrazine by water prior to atrazine desorption from the silica surface is also possible; solvation by water weakens the atrazine–silanol interaction.

The chloroform and acetonitrile experiments help to further elucidate the adsorption mechanism since these solvents have different hydrogen bond affinities. Chloroform, is a hydrogen donor whereas acetonitrile is a hydrogen acceptor [48,49]. The chloroform–stirred silica surface spectrum (Fig. 4h) shows an increase in the intensity of the free silanol peak relative to the adsorption spectrum (Fig. 4e). However, the free silanol signal is $\sim 75\%$ of the peak intensity of the pure solvent spectrum (Fig. 4b). In this experiment (Fig. 4b) the silica surface was exposed to neat chloroform for $\sim 10 \text{ s}$, while in the atrazine desorption experiment (Fig. 4h), the silica surface was in contact with chloroform for at least an hour. A weak and broad band below 3000 cm^{-1} is observed after water stirring (Fig. 4g) in addition to an increase in the $3000\text{--}3600 \text{ cm}^{-1}$ region. These findings are consistent with water vapor being adsorbed to the surface as revealed in Fig. 2. Similar to the water–stirred silica surface (Fig. 4g), the chloroform–stirred silica surface spectrum (Fig. 4h) reveals an intensity reduction of the CH stretching peaks and the NH region. These observations are consistent with atrazine desorption. The reappearance of the free silanol peak after chloroform stirring and the fact that the CH peak intensity was reduced confirm that atrazine was weakly bound through the surface silanol groups. The acetonitrile experiments (Fig. 4c, f, and i) show the same behavior as that for the chloroform experiments (Fig. 4b, e, and h), except that the free silanol peak intensity is recovered by 50% after atrazine desorption. As discussed above, interfacial water may be involved in mediating atrazine desorption in both organic solvents since these solvents and the silica surface can absorb and adsorb water, respectively [23]. Acetonitrile, a highly water soluble solvent is expected to absorb

more water molecules from the gas phase relative to chloroform [50]. High water content in acetonitrile could explain the high intensity in the 3400 cm^{-1} band and the low intensity of the free silanol peak.

Similar to the water, the chloroform and acetonitrile experiments reveal adsorption via the surface silanol sites. Desorption in all three cases occurs easily confirming physisorption. Possible desorption mechanisms are the molecular displacement of atrazine by the solvent molecules at the silanol sites, and/or, a stronger interaction of atrazine with the solvent compared to that with the silanol sites enabling desorption. The water present on the silica surface competes successfully against atrazine for the surface silanol groups. Chloroform and acetonitrile are less successful against atrazine when competing for surface sites due to the lower affinity of these solvents for the silanols. However, it is clear that these solvents act as agents for atrazine adsorption, yet, are also effective at facilitating atrazine desorption.

In the environment, where the surface of silica is typically fully hydrated, the driving force for adsorption of poorly water-soluble compounds, such as atrazine, is the expulsion of these compounds from the aqueous phase due to the hydrophobicity effect [3]. During our experiments, the silica surface adsorbs water molecules from the ambient air, generating a partially hydrated surface. Thus, a comparable driving force is expected to be present during the adsorption of atrazine to the silica surface from the aqueous solution.

In summary, the air–silica interface before, during, and after adsorption of water, chloroform, acetonitrile, and atrazine was investigated using a highly sensitive surface vibrational spectroscopy. Atrazine and water adsorption via the surface silanol sites was observed. Adsorption of chloroform and acetonitrile was weaker than that observed with water. The ease of atrazine desorption suggests that the binding is through a weak physisorption mechanism. Molecular displacement and solvation are suggested mechanisms for atrazine desorption. It is suggested that once atrazine is adsorbed onto the inorganic fraction of soils (in the absence of organics and metals), it is easily desorbed. Consequently, atrazine is expected to be highly mobile in this media.

Acknowledgments

We gratefully acknowledge funding from the National Science Foundation and the Department of Energy (DOE-BES DE-FG02-04ER15495). We also thank Dr. Louise Criscenti for helpful discussions.

Appendix A. Supplementary material

VSGF spectra under sps, ppp, and pss combinations, details on the calculations of the free silanol orientation analysis and thermodynamic parameters are found in the online version. Supplementary data associated with this article can be found, in the online version, at doi:10.1016/j.cplett.2009.10.056.

References

[1] I.I. Mikhaleenko, V.D. Yagodovskii, *Russ. J. Phys. Chem.* 79 (2005) 1363.

- [2] H.A. Al-Abadleh, V.H. Grassian, *Surf. Sci. Rep.* 52 (2003) 63.
 [3] R.P. Schwarzenbach, P.M. Gschwend, D.M. Imboden, *Environmental Organic Chemistry*, John Wiley and Sons, New Jersey, 2003.
 [4] S.M. Miller, C.W. Sweet, J.V. Depinto, K. Hornbuckle, *Environ. Sci. Technol.* 34 (2000) 55.
 [5] E. Barriuso, U. Baer, R. Calvet, *J. Environ. Qual.* 21 (1992) 359.
 [6] R.K. Iler, *The Chemistry of Silica: Solubility, Polymerization, Colloid and Surface Properties, and Biochemistry*, John Wiley and Sons, Wiley-Interscience Publication, New York, 1979.
 [7] H.E. Bergna, W.O. Roberts (Eds.), *Colloidal Silica: Fundamentals and Applications*, CRC Press/Taylor and Francis, Boca Raton, FL, 2006.
 [8] S. Ong, X. Zhao, K.B. Eisenthal, *Chem. Phys. Lett.* 191 (1992) 327.
 [9] X. Zhao, S. Ong, H.-F. Wang, K.B. Eisenthal, *Chem. Phys. Lett.* 214 (1993) 203.
 [10] C.T. Konek, M.J. Musorrafiti, H.A. Al-Abadleh, P.A. Bertin, S.T. Nguyen, F.M. Geiger, *J. Am. Chem. Soc.* 126 (2004) 11754.
 [11] A.L. Mifflin, K.A. Gerth, B.M. Weiss, F.M. Geiger, *J. Phys. Chem. A* (2003) 6212.
 [12] W. Tao, Y.R. Shen, *Phys. Rev. Lett.* (2008) 016101(1).
 [13] D. Langmuir, *Aqueous Environmental Geochemistry*, Pearson Education, Upper Saddle River, New Jersey, 1997.
 [14] L.T. Zhuravlev, *Colloids Surf. A* 173 (2000) 1.
 [15] Y. Duval, J.A. Mielczarski, O.S. Pokrovsky, E. Mielczarski, J.J. Ehrhardt, *J. Phys. Chem. B* 106 (2002) 2937.
 [16] N. Sahai, D.A. Sverjensky, *Geochim. Cosmochim. Acta* 61 (1997) 2801.
 [17] W. Stumm, J.J. Morgan, *Aquatic Chemistry: An Introduction Emphasizing Chemical Equilibria in Natural Waters*, John Wiley and Sons, New York, 1981.
 [18] Q. Du, E. Freysz, Y.R. Shen, *Phys. Rev. Lett.* 72 (1994) 238.
 [19] H.C. Allen, N.N. Casillas-Ituarte, M.R. Sierra-Hernandez, X. Chen, T.C.Y. Tang, *Phys. Chem. Chem. Phys.* 11 (2009) 5538.
 [20] M.C. Messmer, J.C. Conboy, G.L. Richmond, *J. Am. Chem. Soc.* 117 (1995) 8039.
 [21] I. Li, J. Bandara, M.J. Shultz, *Langmuir* 20 (2004) 10474.
 [22] L.M. Levering, M.R. Sierra-Hernández, H.C. Allen, *J. Phys. Chem. C* 111 (2007) 8814.
 [23] M.C. Henry, E.A. Piagessi, J.C. Zesotarski, M.C. Messmer, *Langmuir* 21 (2005) 6521.
 [24] V. Ostroverkov, G.A. Waychunas, Y.R. Shen, *Chem. Phys. Lett.* 386 (2004) 144.
 [25] C. Schnitzer, S. Baldelli, M.J. Shultz, *J. Phys. Chem. B* 104 (2000) 585.
 [26] J.P. Gallas, J.C. Lavalley, A. Burneau, O. Barres, *Langmuir* 7 (1991) 1235.
 [27] B.A. Morrow, A.J. McFarlan, *Langmuir* 7 (1991) 1695.
 [28] Y.R. Shen, *The Principles of Nonlinear Optics*, John Wiley and Sons, New York, 1984.
 [29] R.S. McDonald, *J. Am. Chem. Soc.* 79 (1957) 850.
 [30] V.I. Lygin, *Russ. J. Gen. Chem.* 71 (2001) 1368.
 [31] G. Vigil, Z. Xu, S. Steinberg, J. Israelachvili, *J. Colloid Interf. Sci.* 165 (1994) 367.
 [32] Y.R. Shen, V. Ostroverkov, *Chem. Rev.* 106 (2006) 1140.
 [33] J. Smith, C.D. Cappa, K.R. Wilson, R.C. Cohen, P.L. Geissler, R.J. Saykally, *Proc. Natl. Acad. Sci.* 102 (2005) 14171.
 [34] M. Sovago, R.K. Campen, G.W.H. Wurpel, M. Muller, H.J. Bakker, M. Bonn, *Phys. Rev. Lett.* 100 (2008) 173901(1).
 [35] D.B. Asay, S.H. Kim, *J. Phys. Chem. B* 109 (2005) 16760.
 [36] A.L. Goodman, E.T. Bernard, V.H. Grassian, *J. Phys. Chem. A* 105 (2001) 6443.
 [37] A. Bogdan, M. Kulmala, *J. Colloid Interf. Sci.* 191 (1997) 95.
 [38] K. Klier, J.H. Shen, A.C. Zettlemoyer, *J. Phys. Chem.* 77 (1973) 1458.
 [39] S. Wendt, M. Frerichs, T. Wei, M.S. Chen, V. Kempter, D.W. Goodman, *Surf. Sci.* (2004) 107.
 [40] D.W. Sindorf, G.E. Maciel, *J. Am. Chem. Soc.* 105 (1983) 1487.
 [41] N. Ji, V. Ostroverkhov, C.S. Tian, Y.R. Shen, *Phys. Rev. Lett.* 100 (2008) 096102(1).
 [42] E. Tyrode, M. Johnson, S. Baldelli, C. Leygraf, M.W. Rutland, *J. Phys. Chem. B* 109 (2005) 329.
 [43] M.P. Colombini, R. Fuoco, S. Giannarelli, L. Pospíšil, R. Trsková, *Microchem. J.* 59 (1998) 239.
 [44] M. Windholz (Ed.), *The Merck Index: An Encyclopedia of Chemicals and Drugs*, Merck, Rahway, NJ, 1976.
 [45] M.L. Zaki, M.A. Hasan, F. Al-Sagheer, L. Pasupulety, *Colloids Surf. A* 190 (2001) 261.
 [46] T.J. Dines, L.D. MacGregor, C.H. Rochester, *J. Colloid Interf. Sci.* 245 (2002) 221.
 [47] G. Wellhouse, W. Bleam, *Environ. Sci. Technol.* 27 (1993) 494.
 [48] M.H. Abraham, P.L. Grellier, D.V. Prior, P. Duce, *J. Chem. Soc. Perkin Trans. 2* (1989) 699.
 [49] M.H. Abraham, P.L. Grellier, D.V. Prior, J.J. Morris, P.J. Taylor, *J. Chem. Soc. Perkin Trans. 2* (1990) 521.
 [50] D.R. Lide (Ed.), *CRC Handbook of Chemistry and Physics*, CRC Press/Taylor and Francis, Boca Raton, FL, 2009.